Research Report

2014-17

Novel Field Weakening Technique for Surface Mounted Permanent Magnet Machine using Current Regulated Voltage Source Inverters

S. Atiq, T.A. Lipo*, B. Kwon

Electronic Systems Engineering
Hanyang University
Ansan-si, Gyeonggi-do, Korea

*Electrical Engineering
University of Wisconsin-Madison
Madison, WI 53706, USA

WEMPEC

Wisconsin
Electric
Machines &
Power
Electronics
Consortium

University of Wisconsin-Madison
College of Engineering
Wisconsin Power Electronics Research Center
2559D Engineering Hall
1415 Engineering Drive
Madison WI 53706-1691

Novel Field Weakening Technique for Surface Mounted Permanent Magnet Machine using Current Regulated Voltage Source Inverters

***Abstract*— Field weakening control is a key technique for high speed operation of electrical machines. A novel Current Regulated Voltage Source Inverter (CRVSI) operation strategy is adopted in this paper to achieve high speed operation from Surface Mounted Permanent Magnet Synchronous Motor (SMPMSM). This strategy avoids any kind of previously proposed winding switching and achieves same benefits of high flux weakening. Machine operation is divided into two modes: two 3-phase CRVSI operation and three single phase CRVSI operation. During first mode of operation machine can be operated at maximum torque conditions as well as d-axes current control is applied for first stage of flux weakening. In second mode of operation, when machine reaches its constant power operation limit, CRVSIs operation is modified. Three 1-phase CRVSI are established such that machine operation reverts to achieve unity internal power factor at the elevated speed. Suitability of suggested current flow paths for the proposed topology is supported by inductance variation calculations. Furthermore effect of slot per pole per phase configuration on this flux weakling topology is discussed. Initial experimental results are provided to validate the simulation results.**

Keywords—windng switching; Current Regulated Voltage Source Inverter; Field Weakening; Internal Power Factor

I. Introduction

Surface Mounted Permanent Magnet Synchronous Motors (SMPMSM) have numerous applications due to their suitable characteristics like high power density, high efficiency, high torque to inertia ratio, etc. One of their suitable applications is traction like electric and hybrid vehicles. However high speed operation in these applications is limited by inverter voltages. To deal with this inverter voltage limitation, field weakening becomes inevitable to reduce the net stator flux linkage and hence the back emf of the machine. Flux of the machine can be reduced either by applying negative d-axis currents or utilizing some other technique such as winding switching

A number of field weakening control strategies have been addressed in the literature [1]-[11]. A brief overview of these techniques is presented in this section. In [1] the authors have proposed flux weakening based upon q-axis and d-axis current control and discussed maximum speed limits for current tracking depending upon dc link voltages. Authors in [2] have used closed loop control of phase voltage magnitude to calculate d-axis reference for flux weakening. This algorithm is robust without any steady state error. However this algorithm has sluggish response for torque changes and can even result in unstable operation. In [3] authors have presented the transient response and design considerations for the scheme described in [2]. Reference [4] has described the performance degradation due to high harmonic contents in overmodulated six step PWM inverter mode. Reference [5] presents the remedial strategy for the problem indicated in [4]. Authors in [6] have proposed a robust flux weakening control strategy in closed form solution of available maximum torque to eliminate the gradual adjustment by feedback mechanism to get improved response and stability. Field weakening technique that remains indifferent to some parameters changes and operates at minimum copper loss strategy is proposed in [7]. An Infinite Constant Power Speed Ratio (CPSR) is presented in [8]. There is strong coupling between magnetization component and torque component of currents at high speed. Authors in [9], [10] and [11] have exploited this fact to achieve flux weakening capabilities of Interior Permanent Magnet Machine.

On the other hand some authors have used winding switching techniques and/or multiple poles winding for variable speed operation of the machines. Authors in [12] have used series to parallel winding switching to achieve two speed operation of the motor. Reference [13] concerns changing pole numbers for multiple speed ranges. Authors in [14] have proposed a new winding switching strategy to achieve flux weakening. A central connection is established at the center of three phases of winding and motor is fed through two equal size inverters at both ends. Current in one half of the machine reverses its direction at winding switching thus reversing flux in that half and resulting overall subtractive flux from two halves of the machine. However, winding switching at full load condition may result in a severe transient state that is not favorable for many applications.

A novel control strategy is introduced in this paper to avoid winding switching. Instead of winding switching, inverter operation is modified to control the current flow in windings and achieve winding switching benefits without physically switching the winding. Suitability of the proposed currents path for flux weakening is also validated using winding inductance calculations. Flux weakening capability of the machine with different slots per pole per phase (SPP) is also investigated in this work. Finally basic experimental results are provided to validate the flux weakening strategy.

II. Proposed Topology

SMPMSM is normally considered to be a poor candidate for flux weakening control due to their low inductance values. Authors in [14] have proposed a new concept concerning flux weakening. Double layer distributed windings as shown in Fig.1

are proposed in [14] that can be switched to reduce the flux of the machine. A central connection is implemented that splits the main winding into two equal sub windings namely ABC and XYZ in this paper. Windings ABC and XYZ are fed with two independent inverters. Current entering at dotted end of the winding is assumed to generate positive MMF while current leaving the dotted end is assumed to generate negative MMF. Before winding switching, currents are entering at dotted ends of both half windings and flux from both halves is positive. After winding switching current enters at dotted end of one half and leaves at the dotted end of the other half winding [14]. Thus half of the winding generates positive flux while other half generates negative flux and net air gap flux is reduced, allowing motor to operate at higher speed. Fig. 2 and Fig .3 are taken from [14] to demonstrate the principle.

Although winding switching achieves the flux weakening objective very well, winding switching operation at high speed gives rise to transients that is not favorable for the smooth operation of the motor. Furthermore machine in [14] cannot keep power constant for the entire high speed constant power operation. In this paper instead of using winding switching to change winding configurations, inverter operation is modified to achieve flux weakening. Switching action is eliminated to avoid unwanted transient states during the machine operation. Drive circuit for the proposed idea contains twelve semiconductor switches and required control circuitry. Twelve semiconductor switches can constitute two 3-phase bridges or three 1-phase bridges. Initially machine is operated with two 3-phase CRVSI feeding current at the dotted end of both windings. Machine operation in this mode will be called mode-1 operation in this paper. For the flux weakening operation, instead of switching windings CRVSIs operation is

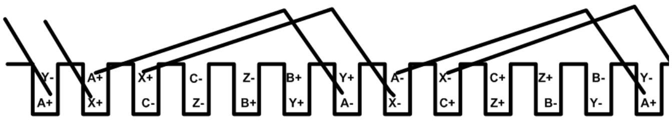

Fig. 1. Basic structure of two layer lap winding.

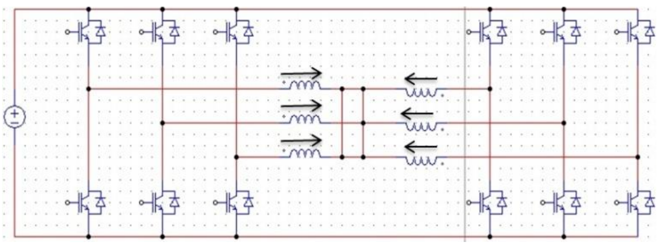

Fig. 2. Winding configuration before switching.

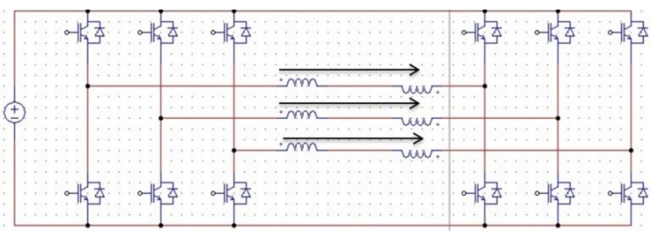

Fig. 3. Winding configuration after winding switching.

modified. Two CRVSIs operating in 3-phase mode are now connected in three 1-phase CRVSIs mode as shown in fig.4. This will be called mode-2 operation in this paper. Current is forced to move in from the dotted end of the ABC winding and out from the dotted end of the XYZ winding. The d-axes current is removed and the machine reverts to unity internal power factor operation but at the elevated speed at the mode switching instant. Thus, mode-2 operation results in deep flux weakening operation of the machine by applying again d-axes current from zero up to the maximum allowed limit and achieving further flux weakening. Switches encircled in red in Fig.4 constitute one single phase bridge that forces current to enter at dotted end in phase A from ABC winding and leave at dotted end in phase X from XYZ winding. Similar explanation holds for switches encircled in blue and green those constitute remaining two single phase bridges. This operation results in a positive MMF from ABC winding and negative MMF from XYZ winding. The net MMF is the difference of MMFs from two windings. Figure 5 and Fig.6 show the MMF diagram of the machine during its normal operation i.e. operation in mode-1 and mode-2 that is flux weakened mode of operation.

This operation is achieved by opening the central connection of the winding in [14]. In this paper single phase current regulator is formed across each phases of the two windings to force the current to produce flux weakening without opening the central connection.

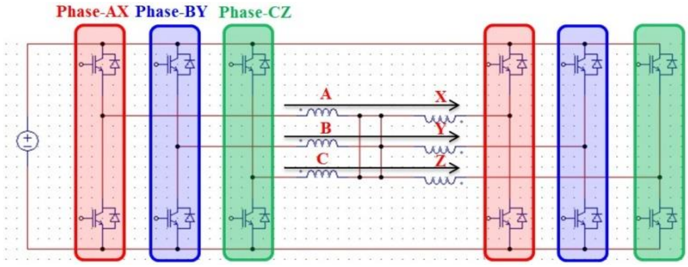

Fig. 4. Proposed drive topology.

Fig. 5. MMF of the machine during its operation in mode-1

Fig. 6. MMF of the machine during its operation in mode-2

III. System Analysis

In this section machine behavior with respect to back EMF and winding inductances is analyzed during both operation modes. Back EMF analysis is associated with high speed operation of the machine. The winding inductance analysis helps to understand the current flow paths when machine switches its operation from mode-1 towards mode-2 and demonstrates the suitability of proposed current paths in terms of current path impedances. Also constant power capability of the machine is investigated in terms of ratio between back EMF and synchronous reactance of the machine.

A. Analysis of the EMF behavior of the Machine

In this proposed winding configuration electrical angle between two sub windings ABC and XYZ determines the magnitude of the flux weakening. Different arrangements of Slots per Pole per Phase (SPP) results in different angles between two sub windings and hence affects the flux weakening capability of the machine that is discussed in the subsequent section.

Flux weakening capability of machine with SPP equal to two is analyzed. Two sub windings ABC and XYZ are 30 degree apart electrically in this configuration. EMF equations for ABC and XYZ windings are given in (1)-(6).

$$E_a = E\sin(\omega_e t - \delta) \quad (1)$$

$$E_b = E\sin(\omega_e t - 2\pi/3 - \delta) \quad (2)$$

$$E_c = E\sin(\omega_e t + 2\pi/3 - \delta) \quad (3)$$

$$E_x = E\sin(\omega_e t - \pi/6 - \delta) \quad (4)$$

$$E_y = E\sin(\omega_e t - 5\pi/6 - \delta) \quad (5)$$

$$E_z = E\sin(\omega_e t + \pi/2 - \delta) \quad (6)$$

where

E Induced emf with subscript representing respective phases

δ Angle between rotor and stator magnet field

EMF of the machine from phase A and Phase-X are positive during its operation such that (7) and (8) are obtained

$$E_{AX\_mode-1} = E\sin(\omega_e t - \delta) + E\sin(\omega_e t - \pi/6 - \delta) \quad (7)$$

$$E_{AX\_mode-1} = 1.93E\sin(\omega_e t - \pi/12 - \delta) \quad (8)$$

Where, E_{AX_mode-1} is net EMF of phase-A and phase-X during its operation in mode-1. When machine switches to mode-2, EMF induced by phase-X becomes negative while EMF induced by phase-A remains positive such that (9) and (10) are obtained

$$E_{AX\_mode-2} = E\sin(\omega_e t - \delta) + E\sin(\omega_e t - \pi/6 - \delta) \quad (9)$$

$$E_{AX\_mode-2} = 0.51E\sin(\omega_e t - 5\pi/12 - \delta) \quad (10)$$

Where, E_{AX_mode-2} is net EMF of phase-A and phase-X during mode-2 operation. Ratio of E_{AX_mode-1} to E_{AX_mode-2} gives the flux weakening achieved while switching from mode-1 to mode-2. Magnitude of field weakening achieved is given by (11) and (12)

$$E_{weakened} = |E_{AX\_mode-1} / E_{AX\_mode-2}| \quad (11)$$

$$E_{weakened} = 3.73 \quad (12)$$

Equation (12) demonstrates that EMF of the machine reduced to about 3.73 times while going from mode-1 to mode-2 operation. This result shows that speed of the machine can be increased by 3.73 times the base speed while switching from mode-1 to mode-2. When mode-2 starts machine operation reverts to unity internal power factor at a speed of 3.73 times the base speed. Again negative d-axis current is applied for the further flux weakening. Overall flux extended speed range of machine will be about 6.46 times the base speed (13).

$$S_{final} = (3.73 + (3.73 - 1))S_{rated} \quad (13)$$

where S_{final} Final achievable speed of the machine

S_{rated} Rated speed of the machine

Table I shows the SPP combination and the flux weakening capability of the proposed two layer lap winding. As SPP of the machine increases angle between ABC and XYZ sub windings decreases and flux weakening capability of the machine increases.

TABLE I. SPP COMBINATION AND FLUX WEAKENIG CAPABILITY

SPP	Angle between ABC&XYZ	Flux Weakening Ratio	Achievable speed multiple of base speed
1	60°	1.732 : 1.000	1.732
2	30°	1.732 : 0.517	3.35
3	20°	1.732 : 0.347	4.99
4	15°	1.732 : 0.261	6.63

B. Analysis of the winding inductances

Machine in mode-2 is controlled with three single phase CRVSIs. Each CRVSI is applied across nearby phases (electrical degrees) of ABC and XYZ winding. This establishes current flow paths AX, BY and CZ respectively. Current paths from phase A to phases B, C, X, Y and Z exist as shown in Fig. 7. However the proposed current flow paths for flux weakening operation is through phase A and X.

In this section winding inductances for all existing paths with respect to phase A are calculated using winding function theory [15]. Equation (14) is used to calculate self-inductances of the available current paths.

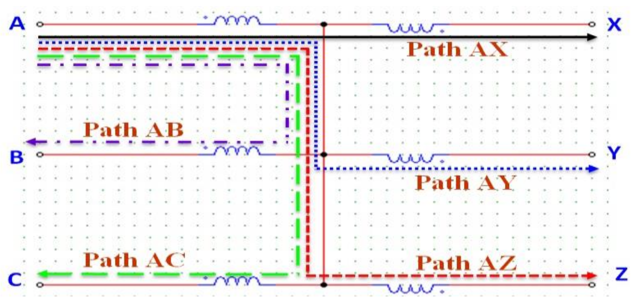

Fig. 7. Possible current flow paths from phase A.

$$L_{AA} = \frac{\mu_0 r l}{g}\int_0^{2\pi} N_A^2(\emptyset)\,d\emptyset \quad (14)$$

where,

L_{AA} Self-inductance of phase A (H)

μ_o permeability of air (H/m)

l Active length (m)

g Air gap length (m)

N_A Number of turns

The self-inductance of each phase A, B, C, X, Y and Z in mode-1 using (14) is calculated to be 5π/12. When machine switches to mode-2 self-inductance of each phase AX, BY and CZ reduces to π/6. Self-inductances of all possible current paths from phase-A are calculated and are given in Table.II. This table shows that the minimum impedance path is through phase AX. Similarly for phase B it will be BY and for phase C, CZ will be the minimum impedance path. This demonstrates the natural tendency of current flow through phases AX, BY and CZ as current tries to flow through minimum impedance path. Moreover currents in all three resultant phase AX, BY and CZ is controlled such that all three phases maintain three phase symmetrical and there is no current flowing from the central neutral point to another phase. Even if some imbalance occurs, this inductance table shows that for the worst case 1/3 of the rated current will deviate from the desired path because impedance of all other paths is at least 3 times higher than the proposed path.

TABLE II. AVAILABLE CURRENT FLOW PATHS FROM PHASE-A

No.	Available Path	Self-Inductance
1	AB	3π/6
2	AC	3π/6
3	AX	π/6
4	AY	9π/6
5	AZ	5π/6

C. Analysis of constant power capability

It should be noted that machine being considered for this control should be capable of keeping power constant at an elevated speed that is theoretical determined by this topology i.e. 3.73 times the base speed. An extended constant power region is a function of internally generated voltages and the synchronous reactance of the machine [16]. Five machine models are developed and tested for constant power region capability with rated power of 4920W. For the proposed topology with SPP =2, machine having constant power region of 3.73 times the base speed is sufficient.

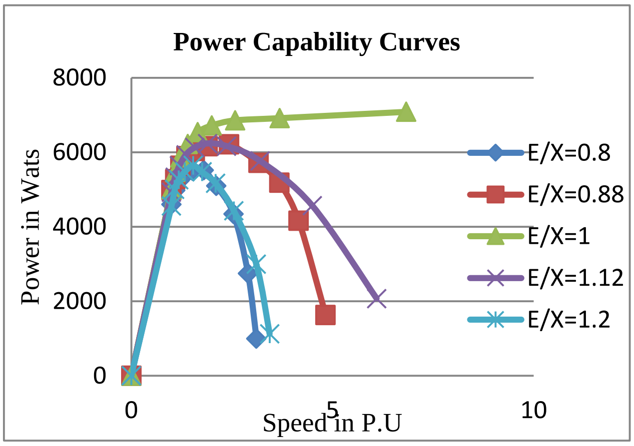

Fig. 8. Power capability curves of the machines with different E/X

Constant power region of machines with E/X =0.8 and E/X=1.2 in Fig.8 is limited to around 2.2times the base speed which do not fulfill the requirement of the proposed topology. Machines with E/X=0.88 and 1.12 have constant power region of about 4 times the base speed that fairly meets the requirement. Machine model with E/X = 1.12 is used for further analysis to verify the effectiveness of proposed topology.

IV. SIMULATION MODEL

A 5-Kw SMPMSM model is developed and has been simulated using Maxwell 2D to demonstrate the effectiveness of the proposed topology. Basic dimensions of the model are given in Table. III. Low price bonded NdFeb magnets are used with permanence of 0.54T. Machine is designed to operate at 1800 rpm with a supply frequency of 60Hz.

TABLE III. SIMULATION MODEL PARAMETER

Parameter	Value	Unit
Stator outer diameter	230	mm
Rotor outer diameter	110	mm
Stack Length	50	mm
Air gap length	1	mm
Magnet type	NdFeB	--
Magnet depth	11	mm
Number of poles	4	--
Number of slots	24	--
Winding inductance per phase	6.9	mH
Synchronous reactance at base speed	13.9	ohm
Base Speed	1800	rpm

V. SIMULATION RESULTS AND DISCUSSIONS

During mode-1 of operation of the machine, machine first operates in constant torque region up to 1800 rpm. After 1800 rpm negative d-axis current is to be applied to further increase the speed of the machine. Speed of the machine increases at the cost of torque of the machine because as d-axis current increases q-axis current decreases in accordance with (15)

$$I_s \geq \sqrt{(I_d^2+I_q^2)} \tag{15}$$

When the machine switches to mode-2 operation, torque of the machine should reduce by same factor as flux of the machine i.e 3.73 times the rated value.

Initially the machine is operated at unity internal power factor in constant torque region for maximum torque. The machine reaches at 1800 rpm at a power of 4921 W. Negative d-axis current is then applied up to 75 degrees until machine reaches 6600 rpm with 7.45 Nm torque. Theoretically mode-2 should start its operation from 6715 rpm with torque of 6.91 Nm. Again negative d-axis current can be applied so that machine reaches at 10270 rpm with 5.36 Nm torque. Figure 9 shows the speed torque characteristics of the machine during mode-1 and mode-2 of operation. When constant power region in mode-1 reaches its limit, machine is switched to mode-2 operation. Mode-2 further extends the speed of the machine (3.73-1) times base speed.

Power capability curve of the machine for mode-1 and mode-2 operation is shown in Fig.10. It is obvious that machine maintains its power above the rated value throughout the extended speed operation region in both mode-1 and mod-2.

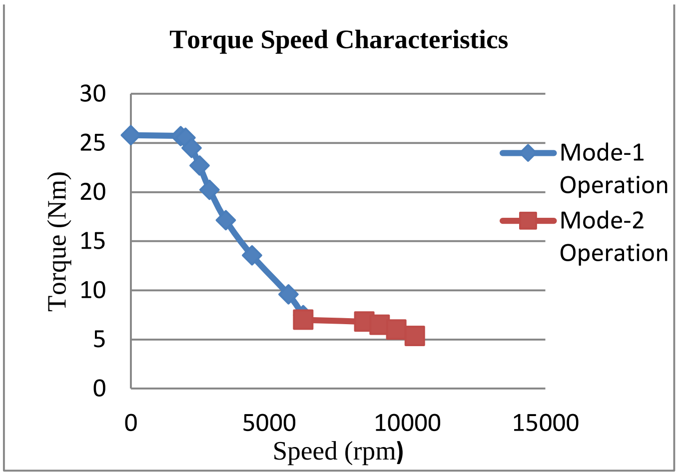

Fig. 9. Speed Torque characteristic curve.

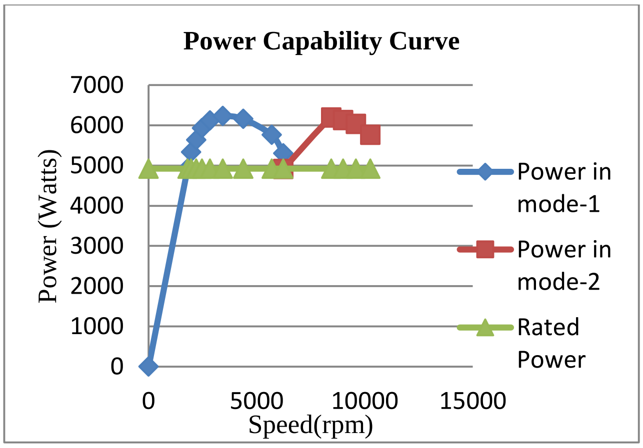

Fig. 10. Power capability curve of the machine for mode-1 and mode-2

VI. Experimental Set Up

For experimental verification of the proposed topology commercially available 2 Kw is being used. Although its power rating is different from the simulation model but this is sufficient to validate the principle of operation and flux weakening range. Figure 11 shows the rotor and stator of this commercially available model. Table IV gives the dimensions of the machine under test. Maximum allowed speed of the machine is 5500 rpm. Keeping in view the mechanical speed limit of the machine, machine is being operated at base speed of 900 rpm. Drive circuit for the machine control is shown in Fig.12. Custom manufactured control board having DSP controller 320F28335 from Texas instrument is being used for

TABLE IV. Experiment motor parameter

Parameter	Value	Unit
Phase resistance	0.25	ohm
D-Axis inductance	1.33	mH
Q-Axis inductance	1.33	mH
Magnet type	NdFeB	--
Maximum allowed speed	5500	rpm
Number of poles	4	--
Number of slots	24	--

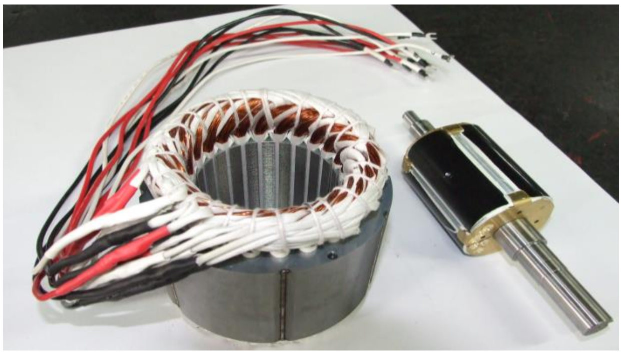

Fig. 11. Rotor and Stator of the machine being used for experiment

Signal processing and control signal generation. SKM75GB128D from Semikron International are used as power IGBTs for inverter circuits. DC link is directly being supplied from controllable DC power supply ES 2000S.

VII. Initial Experiment Results

Initially machine is tested for the back EMF generation in two modes of operation. Machine terminals are left open and machine is rotated at rated speed of 900 rpm through another motor in the test bench. Figure 13 shows the back EMF of the machine during its operation in mode-1 while Fig.14 shows back EMF of the machine for mode-2 operation at rated speed. During mode-1 operation, machine generated 19.66 Vrms which reduces to 5.54 Vrms when machine switches to mode-2 operation. Hence a decrease of 3.55 times while switching from mode-1 to mode-2 operation is measured. Ideally it should reduce 3.73 times but the measured value deviates from theoretical value about 4.83% that is acceptable due to practical limitations of the hardware compared to ideal calculations. Full control of the machine in both modes is under process.

I. Conclusion

Flux weakening operation of SMPMSM has been demonstrated in this paper. Winding switching operation is avoided by modifying the operation of CRVSIs. Three phase operation of two CRVSIs is suggested to drive the machine in mode-1 whereas three single phase mode of operation of CRVSIs is suggested for mode-2. Flux weakening of about

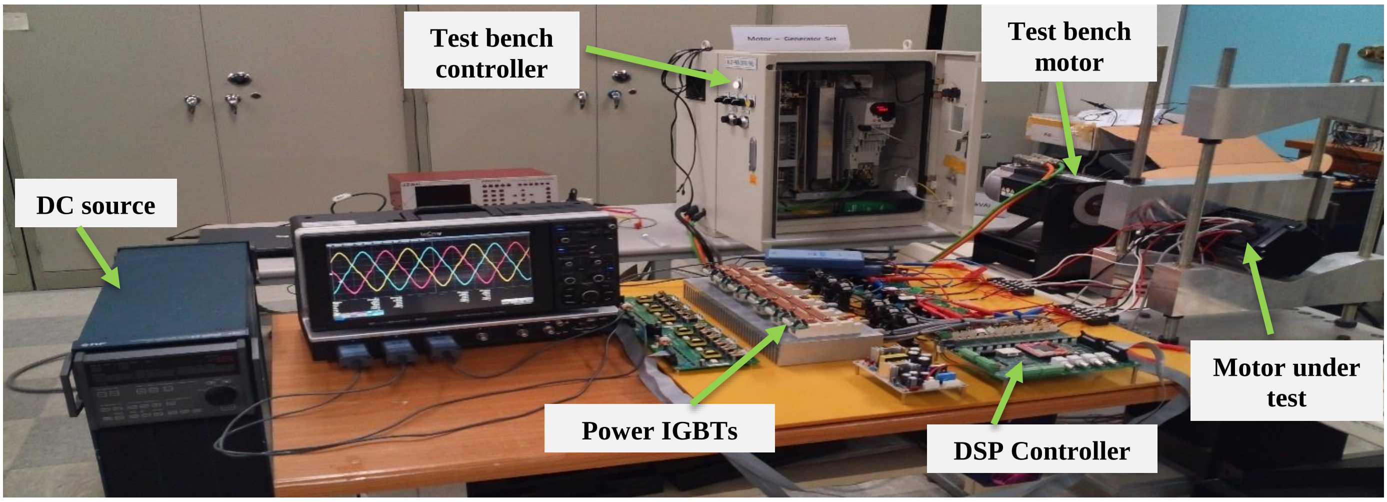

Fig. 12. Experiment setup

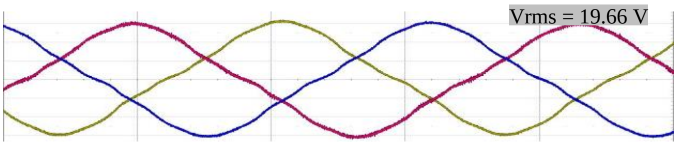

Fig. 13. Back EMF of the machine during mode-1 operation

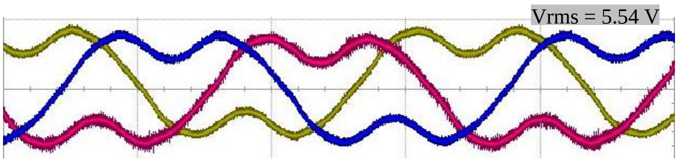

Fig. 14. Back EMF of the machine during mode-1 operation

3.73 times the rated flux is demonstrated when machine switches its operation from mode-1 to mode-2. An elevated speed of about 6.46 times the base speed is achievable with a machine having a normal elevated constant power range of 3.73. Furthermore, from winding inductance calculations, it is also demonstrated that proposed current flow path for achieving flux weakening are the most suitable paths for current flow due to low inductances associated with these paths. Flux weakening capability of the proposed topology with different SPP configuration of the machine is also discussed. Initial experiment results validate the effectiveness of proposed topology.

REFERENCES

[1] S.D.Sudhoff, K.A. Corzine, and H.J. Hegner, "A flux-weakening strategy for current-regulated surface-mounted permanent-magnet machine drives," IEEE Transactions on Energy Conversion, Vol.10, Issue: 3, pp. 431-437, 1995.

[2] D.S. Maric, S.Hiti, C.C.Stancu, J.M.Nagashima, "Two improved flux weakening schemes for surface mounted permanent magnet synchronous machine drives employing space vector modulation," Proceedings of the 24th Annual Conference of the IEEE Industrial Electronics Society, 1998 Vol.1 pp. 508-512.

[3] D.S.Maric, S.Hiti, C.C. Stancu, J.M.Nagashima, D.B. Rutledge, "Two flux weakening schemes for surface-mounted permanent-magnet synchronous drives. Design and transient response considerations," Proceedings of the IEEE International Symposium on Industrial Electronics, 1999, ISIE '99, Vol. 2 pp.673-678

[4] J.Holtz, W. Lotzkat, A. Khambadkone, "On continuous control of PWM Inverters in the overmodulation range including the six-step mode," International Conference on Industrial Electronics, Control, Instrumentation, and Automation IECON 1992, vol.1 pp 307-312.

[5] D. S. Maric, S. Hiti, C. C. Stancu, J. M. Nagashima, and David B. Rutledge, “Robust Flux Weakening scheme for Surface-Mounted Permanent-Magnet Synchronous drives employing an adaptive lattice-structure filter,” Fourteenth Annual Applied Power Electronics Conference and Exposition, APEC '99, vol. 1, 1999, pp. 271-276.

[6] Ching-Tsai Pan , Jenn-Horng Liaw "A robust field-weakening control strategy for surface-mounted permanent-magnet motor drives," IEEE Transactions on Energy Conversion 2005, vol. 20 pp. 701-709.

[7] Shinn-Ming Sue , Ching-Tsai Pan , Yuan-Chuen Hwang, "A new Field-weakening control scheme for Surface Mounted Permanent-Magnet Synchronous Motor Drives," Industrial Electronics and Applications, ICIEA 2007, pp. 1515-1520.

[8] Tae-Suk Kwon ; Seung-Ki Sul, "A novel flux weakening algorithm for surface mounted permanent magnet synchronous machines with infinite constant power speed ratio," Intl Conf on Electrical Machines and Systems,ICEMS 2007 440-445.

[9] Zhu Lei , Xue Shan , Wen Xuhui , Li Yaohua , Kong Liang, "A new deep Field-Weakening strategy of IPM machines based on single current regulator and voltage angle control," Energy Conversion Congress and Exposition (ECCE), 2010, pp 1144-1149.

[10] Taiyuan Hu , Fei Lin , Kezhen Lin , Xiaocun Fang , Zhongping Yang, "Flux-weakening control of PMSM based on single current regulator and variable q-axis voltage," Electrical Machines and Systems (ICEMS), 2012, pp. 1-6.

[11] Yuan Zhang , Longya Xu, M.K.Güven, Song Chi , M. Illindala, "Experimental verification of deep Field Weakening operation of a 50-kW IPM machine by using single current regulator," IEEE Transactions on Industry Applications, 2011. vol.47 pp. 128-133.

[12] Hong Huang, Liuchen Chang, "Electrical two-speed propulsion by motor winding switching and its control strategies for electric vehicles," IEEE Transactions on Vehicular Technology, 1999, vol. 48 pp. 607-618.

[13] K.C. Rajaraman, "Pole-changing motor using π-spread phase windings," Proceedings of the Institution of Electrical Engineers, 1970, vol.117, pp 957-960.

[14] S. Hemmati and T.A. Lipo, “Field Weakening of a Surface Mounted Permanent Magnet Motor by winding switching” International Symposium on Power Electronics, Electrical Drives, Automation and Motion (SPEEDAM), 2012 pp. 736-740.

[15] T.A Lipo, “Analysis of Synchronous Machines,” (book) University of Wisconsin, WisPERC, 2008.

[16] R.F. Schiferl, T.A. Lipo “Power capability of salient pole permanent magnet synchronous motors in variable speed drive applications” IEEE Transactions on Industry Applications 1990, vol.26 pp 115-123

1. Shahid Atiq
Electronic Systems Engineering
Hanyang University
Ansan-si, Gyeonggi-do, Korea
shahidatiq@ hanyang.ac.kr,

2.Thomas A. Lipo
Electrical Engineering
University of Wisconsin-Madison
Madison, WI 53706, USA
lipo@engr.wisc.edu

3. Byung-il Kwon
Electronic Systems Engineering
Hanyang University
Ansan-si, Gyeonggi-do, Korea
bikwon@hanyang.ac.kr